general scheme, the analysis parameters do not require solvent modification, variable injection volumes, or a change in analysis time. The only chromatographic variation is an attenuation change from 0.1 to 0.2 aufs for the 2.5% hydrocortisone formulations.

A variety of hydrocortisone formulations may contain methylparaben and propylparaben as preservatives. Though methylparaben interferes with phenethyl alcohol, benzyl alcohol could be substituted as the internal standard and yield satisfactory chromatographic separation.

REFERENCES

(1) "The United States Pharmacopeia," 20th rev., United States Pharmacopeial Convention, Rockville, Md., 1980, p. 172.

(2) *Ibid*, p. 1212.

(3) H. C. Van Dame, *J. Assoc. Off. Anal. Chem.*, **63**, 1184 (1980).

(4) M. Lanouette and B. A. Lodge, *J. Chromatogr.*, **129**, 475 (1976).

(5) T. Okumura and A. Azuma, *Bunseki Kagaku*, **28**, 235 (1979).

(6) S. Hara and K. Mibe, *Chem. Pharm. Bull.*, **15**, 1036 (1967).

(7) H. S. De Boer, P. H. Lansaat, K. R. Kooistna, and W. J. Van Oort, *Anal. Chim. Acta.*, **111**, 275 (1979).

(8) H. S. De Boer, J. Den Hartigh, and H. H. J. L. Ploegmakers, *ibid.*, **102**, 141 (1978).

(9) A. Y. Taira, *EDRO SARAP Res. Tech. Rep.*, **3**, 243 (1978).

(10) H. S. Boer, P. H. Lansaat, and W. J. Van Oort, *Anal. Chim. Acta*, **116**, 69 (1980).

(11) E. A. Ibraham, A. M. Wahbi, and M. A. Abdel-Salam, *Pharmazie*, **28**, 232 (1973).

(12) *Ibid.*, **28**, 195 (1973).

(13) G. Szepesi and S. Gorog, *Boll. Chim. Farm.*, **114**, 98 (1975).

(14) G. Garzo, M. Blazso, and S. Gorog, *Proc. Conf. Appl. Phys. Chem.*, **2**, 301 (1971).

(15) E. M. Chambaz and E. C. Horning, *Anal. Lett.*, **1**, 201 (1968).

(16) W. L. Gardiner and E. C. Horning, *Biochem. Biophys. Acta*, **115**, 425 (1968).

(17) B. Mahme, W. E. Wilson, and E. C. Horning, *Anal. Lett.*, **1**, 746 (1968).

(18) M. G. Horning, A. M. Moss, and E. C. Horning, *Anal. Biochem.*, **22**, 284 (1968).

(19) J. A. Mollica and R. F. Stursz, *J. Pharm. Sci.*, **61**, 445 (1972).

(20) S. Gorog and P. Horvath, *Analyist (London)*, **103**, 346 (1978).

(21) R. E. Graham, E. R. Biehl, C. T. Kenner, G. H. Luttrell, and D. L. Middleton, *J. Pharm. Sci.*, **64**, 226 (1975).

(22) R. E. Graham and C. T. Kenner, *ibid.*, **62**, 103 (1973).

(23) W. J. Mader and R. R. Buck, *Anal. Chem.*, **24**, 666 (1952).

(24) A. R. Lea, J. M. Kennedy, and G. K. C. Loa, *J. Chromatogr.*, **198**, 41 (1980).

(25) N. W. Tymes, *J. Chromatogr. Sci.*, **15**, 151 (1977).

(26) G. Cavina, G. Moretti, B. Gallinella, R. Alimenti, and R. Barchiesi, *Boll. Chim. Farm.*, **117**, 534 (1978).

(27) J. Q. Rose and W. J. Jusko, *J. Chromatogr.*, **162**, 273 (1979).

(28) S. Shoji and K. Mibe, *Chem. Pharm. Bull.*, **23**, 2850 (1975).

(29) P. A. Williams and E. R. Biehl, *J. Pharm. Sci.*, **70**, 530 (1981).

ACKNOWLEDGMENTS

Presented in part at the APhA Academy of Pharmaceutical Sciences, Newport Beach, Calif. meeting, October 1980.

The authors thank Dancoise Beard, Patricia Loh, Linda O'Shea, and Heidemarie Wierzba for technical assistance.

Synthesis and Evaluation of an ^{111}In-labeled Porphyrin for Lymph Node Imaging

RICHARD VAUM *, NED D. HEINDEL *‡ˣ, H. DONALD BURNS *, JACQUELINE EMRICH*, and NATALIE FOSTER‡

Received October 20, 1981, from the **Department of Radiation Therapy and Nuclear Medicine, Hahnemann Medical College and Hospital, Philadelphia, PA 19102* and the ‡*Center for Health Sciences, Lehigh University, Bethlehem, PA 18015.* Accepted for publication January 18, 1982.

Abstract □ ^{111}In-labeled tetra(4-*N*-methylpyridyl)porphyrin was investigated as a possible lymph node imaging agent. A clinically feasible method for the preparation of this radioactive pharmaceutical was developed from experiments with the synthesis and characterization of the unlabeled complex. The *in vivo* distribution of the compound in Wistar rats was determined as a function of time. Favorable lymph node–blood, lymph node–muscle, and specific lymph node–surrounding tissue ratios were obtained.

Keyphrases □ Porphyrin—^{111}In-labeled, synthesis and evaluation, biodistribution, lymph node imaging, rats □ Imaging, lymph node—^{111}In-labeled porphyrin, synthesis and evaluation, biodistribution, rats □ Biodistribution—^{111}In-labeled porphyrin, synthesis, lymph node imaging, evaluation, rats

The diagnostic imaging methods now being used for evaluating disease in the lymphatic system, oil lymphography and technetium Tc 99m antimony trisulfide colloid lymphoscintigraphy, possess significant inherent limitations. These methods image only those nodal groups that drain the subcutaneous injection site, and thus, require patent lymphatic vessels between the injection site and the nodes to be imaged (1–3). An intravenously administered radiopharmaceutical agent that allows the visualization of all nodal groups with a single injection would be an improvement in the diagnosis of lymph node involvement in malignancy.

BACKGROUND

It has been known since the 1940s that many porphyrins and metalloporphyrins display an affinity for lymphatic and neoplastic tissues when injected intravenously (4, 5). These early studies, however, depended solely upon differential fluorescence to detect the presence of the porphyrin in the target tissue and, consequently, were of limited diagnostic utility. A method is available for introducing indium, an electronic isostere of iron, into porphyrins (6). Two nuclides of that element, indium 111 and indium 113m, would be clinically acceptable from the viewpoint of decay energies, gamma-emission, and half-life for use in *in vivo* diagnostic radiopharmaceuticals. Furthermore, it has been shown that several porphyrins can transport β-emitting nuclides (cobalt 58, zinc 65, and palladium 109) to nodal tissue where their ionizing radiation results in selective nodal ablation and diminished rejection rate for skin homographs in dogs dosed with these radio porphyrins (7–9). It has also been demonstrated that an intravenously administered cobalt 57 derivative of a water-soluble porphyrin developed a tumor–blood ratio of 44:1 at 5 days postdosing in the TCT-4904 rat bladder tumor (10). Sufficient precedent exists to indicate that a soluble indium-labeled porphyrin might be nodal specific. This study reports a facile synthesis for radioactive [^{111}In]tetra(4-*N*-methylpyridyl)porphyrin (I) whose biodistribution in rats illustrates its potential as a radiodiagnostic agent for major nodal systems.

0022-3549/82/1100-1223$01.00/0

© 1982, American Pharmaceutical Association

Table I—Percent Dose per Gram Uptake of I in Rat Tissues [a]

Organ	1 hr	4 hr	24 hr	48 hr
Blood	0.179 ± 0.04	0.097 ± 0.03	0.009 ± 0.00	0.006 ± 0.004
Heart	0.125 ± 0.03	0.077 ± 0.03	0.035 ± 0.00	0.023± 0.01
Lungs	0.360 ± 0.10	0.229 ± 0.06	0.119 ± 0.06	0.076 ± 0.02
Pancreas	0.074 ± 0.02	0.049 ± 0.01	0.043 ± 0.01	0.027 ± 0.004
Spleen	0.260 ± 0.09	0.370 ± 0.12	0.530 ± 0.06	0.517 ± 0.42
Liver	0.177 ± 0.06	0.291 ± 0.13	0.526 ± 0.07	0.334 ± 0.08
Fat pad	0.042 ± 0.01	0.025 ± 0.005	0.058 ± 0.07	0.017 ± 0.005
Muscle	0.045 ± 0.01	0.025 ± 0.01	0.012 ± 0.01	0.009 ± 0.004
Femur	0.183 ± 0.08	0.153 ± 0.07	0.080 ± 0.04	0.040 ± 0.02
Testes	0.053 ± 0.02	0.058 ± 0.02	0.031 ± 0.01	0.036 ± 0.03
Kidneys	2.284 ± 0.68	3.652 ± 1.38	4.963 ± 1.00	3.076 ± 0.64
Adrenals	0.256 ± 0.06	0.214 ± 0.11	0.294 ± 0.29	0.120 ± 0.07
Stomach	0.194 ± 0.04	0.127 ± 0.04	0.067 ± 0.02	0.050 ± 0.01
Intestines	0.096 ± 0.03	0.108 ± 0.04	0.063 ± 0.01	0.040 ± 0.01
Thyroid	0.469 ± 0.78	0.214 ± 0.19	0.356 ± 0.34	0.115 ± 0.14
Brain	0.009 ± 0.005	0.004 ± 0.002	0.019 ± 0.03	0.003 ± 0.002
Node	**1 hr**	**4 hr**	**24 hr**	**48 hr**
Inguinal	0.455 ± 0.47	1.317 ± 1.53	0.707 ± 0.55	0.607 ± 0.30
Aortic bifurcation	0.548 ± 0.48	0.836 ± 1.18	0.647 ± 0.39	1.126 ± 1.21
Superior mesenteric	0.387 ± 0.09	0.476 ± 0.10	0.727 ± 0.28	0.562 ± 0.20
Renal and abdominal	0.442 ± 0.42	0.415 ± 0.69	0.851 ± 1.07	1.116 ± 1.13
Thoracic	0.218 ± 0.17	0.242 ± 0.23	0.333 ± 0.42	0.382 ± 0.41
Axillary	0.234 ± 0.07	0.216 ± 0.09	0.458 ± 0.32	0.371 ± 0.03
Cervical	0.291 ± 0.10	0.240 ± 0.08	0.353 ± 0.34	0.384 ± 0.27
Total nodes	0.368 ± 0.12	0.535 ± 0.41	0.582 ± 0.20	0.650 ± 0.34

[a] Each figure is the average of five animals normalized for a 500-g rat.

EXPERIMENTAL

The reactants, indium chloride[1], [^{111}In]indium chloride[2], and tetra(4-*N*-methylpyridyl)porphyrin tosylate salt[3], were obtained commercially. The tosylate salt of the porphyrin was converted to the chloride by passage through an anion-exchange column in the chloride form and the tetra(4-*N*-methylpyridyl) porphyrin chloride (II) used in all subsequent syntheses. UV spectra were obtained on a UV-visible spectrophotometer[4] in aqueous solution. Combustion analyses were performed by a microanalytical laboratory[5].

Synthesis of Indium Tetra(4-*N*-methylpyridyl)porphyrin—Indium chloride (66.0 mg, 0.30 mmole) was dissolved in 2.0 ml of 0.05 *N* HCl. In a 3.0-ml capped vial, 0.02 ml of this solution was evaporated to dryness under nitrogen in a 115° oil bath. Tetra(4-*N*-methylpyridyl)-porphyrin chloride (II) (25.0 mg, 0.03 mmole) was dissolved in 1.0 ml of distilled water and added to the indium chloride residue. This reaction mixture was stirred in a capped vial in a 115° oil bath for 1 hr. The visible spectra of both this reaction mixture and the starting ligand (II) were obtained. The majority of the reaction mixture was retained for elemental analysis. The aliquot portion of the mixture was applied to a 1.0 × 19.0-cm cation exchange column, which had been pretreated by eluting it with 10 ml of 5×10^{-5} *N* HCl. This column was then eluted sequentially with 10 ml of 5×10^{-5} *N* HCl, 30 ml of 5×10^{-4} *N* HCl, 10 ml of 5×10^{-3} *N* HCl, and 100 ml of 5×10^{-2} *N* HCl. The eluate was collected in 180 0.8-ml fractions.

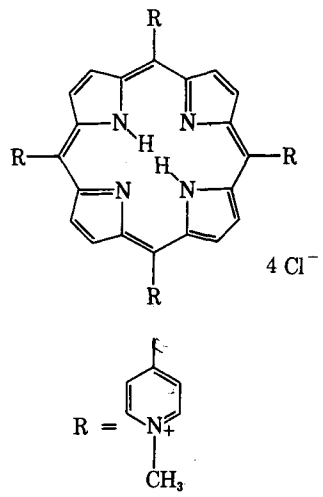

A sample of the porphyrin ligand (II) was passed through an identically prepared column in the same manner. Visible spectra were obtained of representative samples of the colored eluate fractions from both indium tetra(4-*N*-methylpyridyl)porphyrin and the ligand (II) columns. Tubes (130–160 fractions) inclusive from the complex's eluate were then combined, the pH of the resulting solution adjusted to neutrality, and a visible spectrum obtained.

The portion of the original reaction mixture, retained for analysis, was solubilized in 2.5 ml of distilled water and treated with 5 ml of 4 *M* lithium perchlorate. The perchlorate salt precipitated. It was vacuum filtered with a fine frit, washed with cold water, dried under 0.5 torr, transferred carefully with a porcelain spatula (similar perchlorate salts have been reported to explode when rubbed or heated), and a portion subjected to combustion analyses. Chemical yields of the precipitated perchlorates were always in excess of 90% of theoretical. No defined melting point could be observed.

Anal.—Calc. for $C_{44}H_{36}N_8In(ClO_4)_5$: C, 41.12; H, 2.80; N, 8.72. Found: C, 41.28; H, 3.01; N, 8.87.

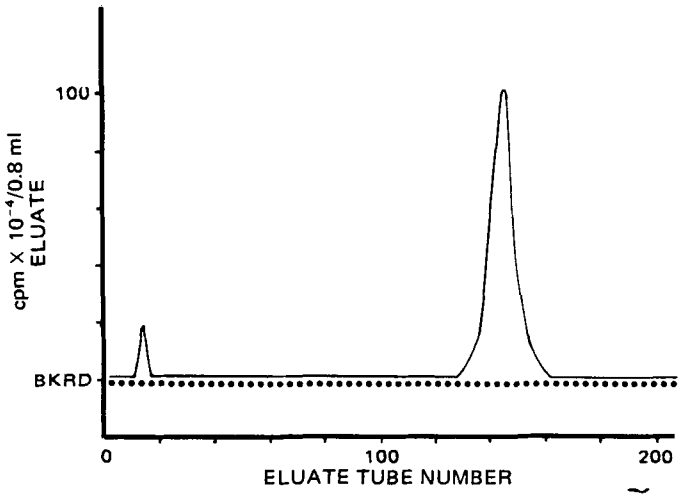

Figure 1—*Elution profile of [^{111}In]indium chloride and of porphyrin complex (I) from cation exchange column. Key: (—) compound I; (. . . .) [^{111}In]indium chloride.*

[1] Alfa Products Thiokol/Ventron Division, lot 041179.
[2] New England Nuclear Corp., carrier free grade as 0.3 ml of a 16-mCi/ml solution in 0.05 *N* HCl.
[3] Man-win Chemical Co.
[4] Beckman, model DK-2A.
[5] G.I. Robertson Microanalytical Laboratory, Florham Park, N.J.

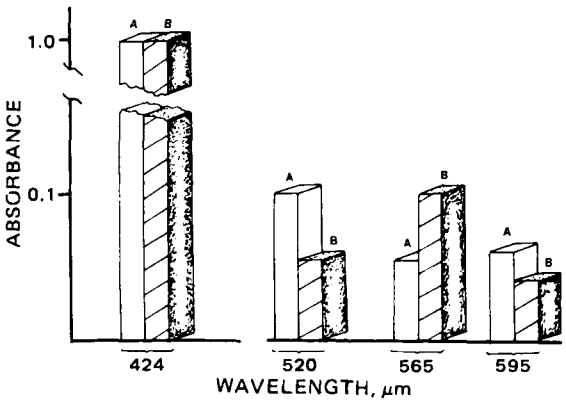

Figure 2—*UV and visible absorption spectra of free porphyrin ligand (II) and of the indium complex of II. Key: (A) indium complex; (B) porphyrin ligand.*

Synthesis of [^{111}In]tetra(4-*N*-methylpyridyl)porphyrin (I)—[^{111}In]indium chloride (3.8×10^{-6} mg, 1.7×10^{-8} mmoles, 1.57 mCi) in 0.05 *N* HCl was evaporated to dryness as described previously for nonradioactive indium chloride. Carrier indium chloride (3.8×10^{-4} mg, 1.7×10^{-6} mmoles) was added to the residue in 100 μl 0.05 *N* HCl, which was once again evaporated to dryness. The ligand (II) (0.14 mg, 1.7×10^{-4} mmoles) in 1.0 ml distilled water was added, and the reaction vial was stirred in a 115° oil bath for 1 hr. The cooled reaction mixture was applied to a cation exchange column prepared identically to those previously described and eluted in the same manner, and the activity of each 0.8-ml fraction was determined. Fractions 130–160 inclusive were combined, and the pH of the resulting solution was adjusted to neutrality by the addition of dilute sodium hydroxide. The neutralized solution was evaporated to a volume appropriate for the animal studies. The effective specific activity of I prepared in this manner was ~9 Ci/mmole as determined by dividing the total indium 111 activity used (1.57 mCi) by the total ligand (II) used (1.7×10^{-4} mmoles).

One microcurie of [^{111}In]indium chloride (2.39×10^{-9} mg, 1.08×10^{-11} mmoles) in 1.0 ml of distilled water was applied to a cation exchange column as previously described for I and was eluted in an identical manner. The activity of every one-tenth fraction plus a tube containing the contents of the eluted column was determined (Fig. 1).

Biodistribution Studies—Biodistribution studies using Wistar rats, average age 6.5 months and average weight 500 g, were carried out over a 4-day period. The animals were sacrificed in groups of 5 at four time periods: 1, 4, 24, and 48 hr. Each rat was injected with 0.2 ml of a 10-μCi/ml concentration of the neutralized solution of I in a caudal vein while under ether anesthesia. Just prior to the end of each time period each rat was again anesthetized with ether and a cardiac puncture was performed. Each rat was then sacrificed by cardiac removal and autopsied. The organs and tissues listed in Table I were removed, weighed, and counted in the gamma scintillation counter. The data for each organ or tissue have been normalized for a rat weighing 500 g, and the percentage of the total injection dose per gram weight has been calculated. The technique for tissue sampling and animal weight normalization has been described previously (11).

RESULTS AND DISCUSSION

Elemental analysis of the indium tetra(4-*N*-methylpyridyl)porphyrin correlated well with the calculated values. Since the amount of I synthesized for this study was too small to be characterized by the same method, another technique for its identification in solution was sought. When II was dissolved in distilled water the resulting solution was dark brown; after being heated with the indium chloride for 1 hr the reaction mixture turned violet in color. This color change was further manifested by a major difference in the visible spectral properties of the complex *versus* the porphyrin ligand. The spectra are compared at equimolar concentrations in Fig. 2. The change in the peak height ratios was used as a convenient tool to detect the complex in the presence of unreacted porphyrin. Cation exchange chromatography was used to isolate I from the crude reaction mixture. This method was capable of demonstrating small quantities of the radioactive complex in the presence of both unlabeled complex and free radioindium. Both the labeled and the unlabeled complexes were shown to elute from the column in the same elution volume (fractions 130–160): the former being demonstrated by a sharp rise in total counts per sample when each tube was examined in a gamma counter (Fig. 1), and the latter being demonstrated by the characteristic color which appeared only in those 30 fractions, and which possessed a visible spectrum identical to that of the complex prior to passing through the column.

Table II—Significant Lymph Node–Background Ratios

	1 hr	4 hr	24 hr	48 hr
Average node–bone	2.0:1	3.5:1	7.3:1	16.3:1
Average node–muscle	8.2:1	21.4:1	48.5:1	72.2:1
Thoracic nodes–heart	1.7:1	3.1:1	9.5:1	16.6:1
Thoracic nodes–blood	1.2:1	2.5:1	37.0:1	63.7:1
Superior mesenteric nodes–intestine	4.0:1	4.4:1	11.5:1	14.0:1

The identification of the labeled complex was considered conclusive when [^{111}In]indium chloride was placed on an identically prepared column, and no counts significantly over the background tissue were detected in the eluate, while the substance of the column was shown to retain all the counts that were applied as the radioactive indium chloride. The final manipulation of I was to neutralize the eluate that contained it with dilute sodium hydroxide before injection. This procedure was examined with the unlabeled complex and was shown to have no effect on the visible spectrum of that compound.

The distribution of I in rats as a function of time is presented in Table I. The percentage of the total injected dose per gram in the lymph nodes is surpassed only by that of the kidneys. More importantly, some node–surrounding tissue ratios, which would be pertinent for imaging both abdominal and thoracic nodal groups, have been expressed in Table II and show considerable prominence of the nodes over background tissue. The nodal groups in these areas are among the most difficult, if not impossible, to image by the best existing techniques, which depend on drainage of the injection site by the lymphatics of the nodes in question.

Earlier studies that reported the node ablation with β-emitting metalloporphyrins did not indicate, however, any property unique to porphyrins which causes their affinity for lymphatic tissue (7–10). It has been theorized in one report that porphyrins and metalloporphyrins are concentrated by tissues with a high mitotic index (4). Bone marrow and duodenal mucosa are two tissues with extremely high turnover rates, and yet in one quantitative study, it was noted that lymph node activity was 16.7 times that of duodenal mucosa and 7.5 times that of bone marrow (7). These data tend to indicate that some quality other than a high mitotic index may be required to explain the localization of these complexes in lymph nodes. It is possible that the complexes localize in the lymph nodes by the mechanism recently proposed for particulate antigens (12). This study showed that colloidal carbon was concentrated in lymph nodes in the region of the high endothelial venules. These unique vessels have been extensively examined (13), and this work suggests that the highly permeable nature of these venules, coupled with the intricate system of hemodynamic controls inherent in the nodal microvasculature, could provide functional lymph node–venous communications. Further study, however, will be required before the porphyrin localization mechanism can be clearly identified.

The potential of I as a diagnostic imaging agent is apparent. The intravenous route of administration would provide an easy and reproducible clinical procedure superior to oil lymphography and to technetium Tc 99m–antimony sulfide lymphoscintigraphy, while the possibility of examining abdominal and thoracic nodal groups by a relatively noninvasive technique would be an invaluable aid in monitoring both neoplastic metastasis and alterations in the immune system in response to a host of other pathologies. Further study of this compound is currently in progress.

REFERENCES

(1) K. D. Kaplan, W. F. Whitmore, and R. F. Gittes, *Invest. Radiol.*, **15**, 34 (1980).

(2) G. N. Ege, *Radiology*, **118**, 101 (1976).

(3) I. Kazem, A. Nedwich, R. Mortel, and T. Honda, *Clin. Radiol.*, **22**, 382 (1971).

(4) F. H. J. Figge, G. S. Weiland, and L. O. J. Manganiello, *Proc. Soc. Exp. Biol. Med.*, **68**, 640 (1948).

(5) D. S. Rassmussen-Taxdal, G. E. Ward, and F. H. J. Figge, *Cancer*, **8**, 78 (1955).

(6) A. D. Nunn, *J. Radioanal. Chem.*, **53**, 291 (1979).

(7) R. A. Fawwaz, H. S. Winchell, F. Frye, W. Hemphill, and J. H. Lawrence, *J. Nucl. Med.*, **10**, 581 (1969).

(8) R. A. Fawwaz, W. Hemphill, and H. S. Winchell, *ibid.*, **12**, 231 (1971).
(9) R. A. Fawwaz, F. Frye, W. D. Loughman, and W. Hemphill, *ibid.*, **15**, 997 (1974).
(10) R. A. Fawwaz, T. S. T. Wang, and P. O. Alderson, *ibid.*, **22**, 50 (1981).
(11) V. R. Risch, A. M. Markow, and T. Honda, in "The Chemistry of Radiopharamceuticals," N. D. Heindel, H. D. Burns, T. Honda, and L. W. Brady, Eds., Masson, New York, N.Y., 1978, p. 145.
(12) J. N. Blau, *Br. J. Exp. Pathol.*, **59**, 558 (1978).
(13) A. O. Anderson and N. D. Anderson, *Am. J. Pathol.*, **80**, 387 (1975).

ACKNOWLEDGMENTS

This investigation was supported in part by PHS Grant CA-22578 awarded by the National Cancer Institute, and by generous support from the Ruth Estrin Goldberg Memorial for Cancer Research and the Elsa U. Pardee Foundation. J. Emrich was supported by the American Cancer Society Biomedical Support Grant IN-146.

Simultaneous Self-Association and Diffusion of Phenol in Isooctane

J. B. DRESSMAN *§, **K. J. HIMMELSTEIN** *‡§x, **and T. HIGUCHI** *

Received June 11, 1981, from the *Department of Pharmaceutical Chemistry, ‡Department of Chemical and Petroleum Engineering, University of Kansas, Lawrence, KS 66045. Accepted for publication January 8, 1982. §Present Address: INTER$_x$ Research Corp., Lawrence, KS 66044

Abstract □ The impact of self-association on mass transport was studied. The model system chosen was the diffusion of phenol through an immobilized layer of isooctane. In the theoretical development, self-associated phenol contributed to diffusion, with the fluxes being interdependent because of the self-association equilibrium. Predictions from theory were then compared with experimental results. It was shown that self-association can significantly affect flux of diffusing species.

Keyphrases □ Phenol—self-association and diffusion in isooctane □ Isooctane—simultaneous self-association and diffusion of phenol □ Diffusion—phenol in isooctane, simultaneous self-association

Associative interactions are of interest to those concerned with pharmaceutics for two reasons. First, associative interactions affect many processes such as dissolution, partitioning, and diffusion, all of which are vitally important to drug delivery. Second, most drugs contain at least one interactive functional group and, thus, are able to participate in associative interactions with many substances found in dosage forms and in the body.

The effects of association and related processes on various aspects of drug delivery have been examined in several studies. Dissolution rate is known to be altered significantly when dissociation reactions (1, 2) or complexation (3) occur within the dissolution layer. It has also been observed that when a diffusing species self-associates (4) or forms micelles (5) there is a pronounced effect on the rate of transport of that substance. Another study (6) has indicated that in a self-associating system, where diffusion of the self-associated species is blocked by its inability to penetrate the membrane used, the observed mass transport behavior can be accounted for by assuming that the compound is transported only in its monomeric form.

Where simultaneous self-association and diffusion occur, the direct application of Fick's laws fails to predict the diffusion rates observed. In the current study, a more comprehensive approach to the theoretical analysis of diffusion under such circumstances is presented. It is postulated that (*a*) by taking into account the interdependence of the fluxes of the associated and unassociated species arising from associative equilibrium within the diffusional layer, (*b*) by applying Fick's laws to each kind of species present, and (*c*) by numerically solving the differential equations derived on this basis, it is possible to predict the mass transport behavior of self-associating systems.

The model system used to test this postulate was one in which phenol was allowed to diffuse from a donor phase of isooctane, through an immobilized layer of isooctane which served as the diffusion layer, into an aqueous receptor phase. Phenol is known to self-associate significantly (>50%) at high concentrations in isooctane (7). This interaction was expected to cause the rate of mass transport into the aqueous phase to deviate markedly from that predicted by simply applying Fick's laws to the overall concentration of phenol present. Using the scheme outlined above, the diffusional behavior of phenol in the model system was predicted mathematically. The predicted results were then compared with the experimental data obtained.

THEORETICAL

Previous studies have shown that when phenol self-associates in isooctane, the dominant species formed is probably the pentamer[1] (7). The equilibrium expression for this interaction has been reported as:

$$5\,P_m \rightleftharpoons P_5$$

where P_m represents monomeric phenol and P_5 represents the pentameric species. The equilibrium constant for this interaction is $K_{1\text{-}5} = 6300\ M^{-4}$ at 25° in isooctane. This model appears to provide an adequate description of self-association of phenol over a wide range of concentrations.

In the present investigation a silanized sintered glass filter with a presilanization pore size range of 4.5–5.5 μm was used to form a diffusional barrier between the donor isooctane and the receptor aqueous phases. Because of the large pore size and equilibration of the filter with the donor phase prior to each experiment, the barrier actually consisted of a layer of isooctane immobilized within the sintered glass filter. As

[1] J. B. Dressman and T. Higuchi, unpublished results.

0022-3549/82/1100-1226$01.00/0
© 1982, American Pharmaceutical Association